THERMAL TIDES IN AN ASSIMILATION OF THREE YEARS OF THERMAL EMISSION SPECTROMENTER DATA FROM MARS GLOBAL SURVEYOR. R. J. Wilson[1], S. R. Lewis[2], and L. Montabone[3], [1]NOAA/Geophysical Fluid Dynamics Laboratory, Princeton, NJ 08542 (John.Wilson@noaa.gov), [2]Department of Physics & Astronomy, The Open University, Walton Hall, Milton Keynes MK7 6AA, UK. [3]Université Paris VI, Laboratoire de Météorologie Dynamique, Paris, France

Introduction. Thermal tides are particularly prominent in the Mars atmosphere with the result that temperature and wind fields have a strong dependence on local solar time (LT). Tides include westward propagating migrating (sun-synchronous) waves driven in response to solar heating and additional nonmigrating waves resulting from zonal variations in the thermotidal forcing. Zonal modulation of forcing can arise from longitudinal variations of the boundary (topography and surface thermal inertia) and radiatively active aerosols (dust and water ice clouds). Nonmigrating tides appear as diurnally varying upslope/downslope circulations within the near-surface boundary layer that, like their migrating counterparts, are also able to propagate vertically to aerobraking altitudes in the lower thermosphere. The Mars Global Surveyor (MGS) Thermal Emission Spectrometer (TES) has yielded atmospheric temperature profiles with unprecedented latitude and longitude coverage that has provided the basis for characterizing the seasonal evolution of tides and stationary waves [1]. However, the twice-daily observations (2 am and 2 pm LT) are insufficient to unambiguously resolve the sun-synchronous tides. Recently the technique of data assimilation has been sufficiently developed for Mars to yield a dynamically consistent set of thermal and dynamic fields suitable for detailed investigations of various aspects of the martian circulations system [2,3,4,5]. We will refer to this data set an the TES Reanalysis, which represents the current best estimate of the evolving state of the martian atmosphere during the MGS mission. The assimilated thermal and dynamical fields provide a means of assessing circulation variability and transport capability reflecting the variability of the actual Mars atmosphere.

Data Assimilation: The data analysis was conducted by assimilating the TES temperature and column dust opacity retrievals into the UK Mars general circulation model (UK-MGCM) to produce a physically self-consistent record of all atmospheric variables archived at a 2 hour interval over the entire MGS mapping period covering roughly three Martian years [2,3]. This data record includes the 2001 global dust storm and several large regional dust storms that occurred during the two other southern hemisphere summer seasons [6].

Three simulations are considered in this study. In addition to the full assimilation, we have examined a simulation using only the assimilated dust field without incorporating the TES temperatures. We have also examined a simulation with a specified dust distribution (Fixed) that roughly mimics a 'typical' MGS year. For this case, the assumed dust specification is zonally uniform.

The assimilated atmospheric fields may be readily decomposed into stationary waves, and eastward and westward propagating thermal tides (and traveling waves). We have examined the seasonal variation of the tide modes. We have looked at the evolving 3-D structure of temperature and geopotential, surface pressure, and near-surface winds. In this presentation we provide a sampling of our results.

Semidiurnal Tide: The latitudinal and vertical structure of the atmospheric response depends on both the period and structure of the forcing and on the efficiency of the atmospheric response to a given forcing. Tide theory indicates that the migrating semidiurnal tide response (S_2) is dominated by a mode with a broad meridional structure and a very long vertical wavelength that efficiently responds to globally integrated dust heating. Figure 1 shows the close correlation between global mean dust opacity and the simulated migrating semidiurnal tide in surface pressure.

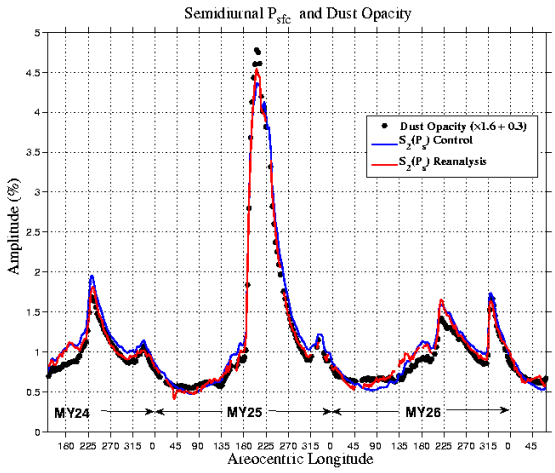

Figure 1. Seasonal variation of the migrating semidiurnal component (S_2) of surface pressure. The amplitude has been normalized by the seasonally-varying diurnal mean surface pressure. The relationship is $S_2 = 1.6\,\tau + 0.3$

This result has been anticipated in previous work [7,8]. The tide response reflects the effects of regional dust storms in the first and third mapping years (MY24 and MY26) and the global dust storm in MY25. The derived relationship between amplitude and opacity suggests that tide forcing associated with heat exchange with the surface accounts for roughly half the tide amplitude during the relatively clear summer solstice seasons. This is confirmed with clear sky and increased dust simulations.

Diurnal Kelvin Wave: Previous MGCM simulations have suggested that a rich mix of eastward and westward tide components is likely present at tropical latitudes and this is supported by our investigation of the TES Reanalysis. The most prominent components of the eastward propagating, diurnal period response are the diurnal Kelvin waves (DK1, DK2,... corresponding to s=-1, -2, ...) which are meridionally symmetric and broad solutions of the Laplace Tidal Equation. DK1 has a vertical structure that closely corresponds to the equivalent barotropic Lamb wave and may be resonantly enhanced [9]. DK1 can be efficiently excited by the interaction of the migrating diurnal tide with zonal wave 2 variations in thermotidal forcing.

The seasonal variation of the eastward propagating, zonal wave 1 component of normalized surface pressure is shown in Figure 2. The broad meridional structure and relative lack of phase variation with latitude is consistent with a Kelvin wave interpretation. The Fixed dust simulation with zonally uniform dust provides a useful reference for indentifying the influences of zonally varying aerosol. Apart from the dust storm periods, the DK1 signal in the Control simulation tracks that of the Fixed simulation quite closely. It is striking that dust storm activity leads to significant increases or decreases in the DK1 signal in both the Reanalysis and Control simulations. The Kelvin wave is sensitive to zonal wave 2 structure in tide forcing and so the effects of a longitudinally modulated dust distribution should results in changes to the wave forcing. As has been discussed in *Zurek* [1976] and [9], Kelvin wave forcing is a result of both topographically-induced dynamical influences as well as zonal variations in the thermal forcing. These contributions typically tend to be out of phase with each other, with the dynamical component of forcing playing the dominant role in establishing the phase of the DK1 response. There is significant DK1 amplification in four out of five of the so-called flushing storm events that were observed during the pre-and post-solstice seasons. We have linked these amplifications to changes in the phase and amplitude of the zonal wave 2 component of the dust distribution. In these cases, the dust component of wave 2 thermal forcing acts to reinforce the contribution from dynamics. It is noteworthy that the L_s = 212° storm in MY26 flushed dust southwards through Isidis towards the north rim of Hellas. The wave 2 dust component of the resulting dust field was out of phase with that associated with the other flushing events and so the DK1 response was suppressed rather than amplified. The contrast between 2001 (MY25) and other years is apparent in the L_s= 220-240° period. Further aspects of the Kelvin wave response to the 2001 global storm event are discussed in [5].

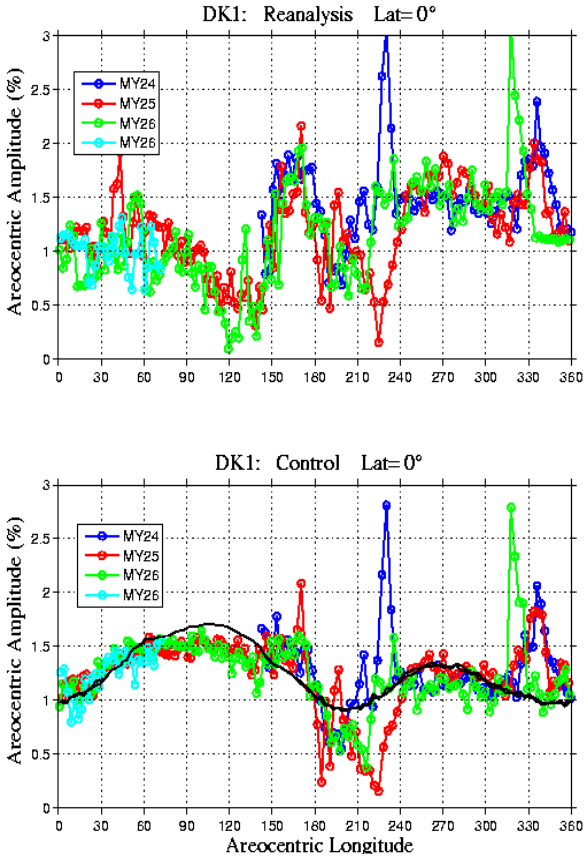

Figure 2. The amplitude of DK1 for the (a) Reanalysis and (b) Control simulations. The black curve shows the DK1 amplitude in the specified (Fixed) dust simulation with zonally-uniform dust mixing ratio. The curves are color coded for MY24-27.

The DK1 response in the Reanalysis and Control simulations are notably different during the NH summer season. We hypothesize that the divergence of the DK1 tide amplitudes after L_s =60 reflects the radiative effects of water ice clouds that are implicit in the 'forcing' imposed by assimilating the TES temperature retrievals and are not accounted for in the Control simulation. It as been argued [10] that radiatively active water ice clouds can account for a cold temperature

bias in the Control simulation in this season. Recent observations and modeling work have shown that nighttime water ice clouds, which have a strong wave 2 distribution, can have a significant radiative impact [11, 12].

Viking Lander Comparison: The time series of surface pressure observations by the two Viking Landers allows for an interesting comparison with the assimilated surface pressures. The Viking Lander 1 tide record shows a high degree of repeatability for 4 Mars years in the L_s=0-130° season which suggests that it is reasonable to directly compare the Reanalysis results with the Viking data. Systematic seasonal variations in phase and amplitude of the diurnal and semidiurnal surface pressure tides at the two Viking Lander sites are consistent with the presence of resonantly enhanced wave 1 diurnal and wave 2 semidiurnal Kelvin waves [9,13].

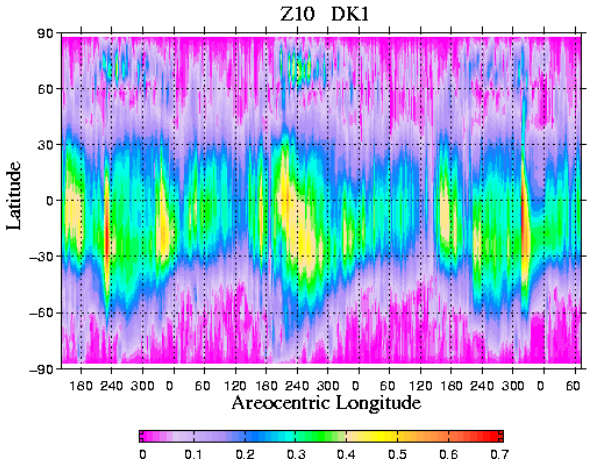

Figure 3. Seasonal variation of the eastward propagating zonal wave 1 component of geopotential height (km) at 0.1 hPa. These results are derived from the TES Reanalysis.

Upper Atmosphere: The seasonal variation of the DK1 component of geopotential height on the 0.1 hPa pressure surface (~35-45 km) is shown in Figure 3. The amplitudes derived from the Reanalysis and Control simulations are quite similar. The short-lived amplification of the DK1 component of geopotential at L_s=315 in MY26 has been detected in Radio Science occultation data [14]. Long vertical wavelengths render diurnal period Kelvin waves less susceptible to thermal dissipation than the shorter westward propagating modes, allowing Kelvin waves to appear prominently in the upper atmosphere [15,16,17]. Hence Figure 3 provides a sense of the seasonal variation in the zonal modulation of density structure that may be anticipated at aerobraking altitudes.

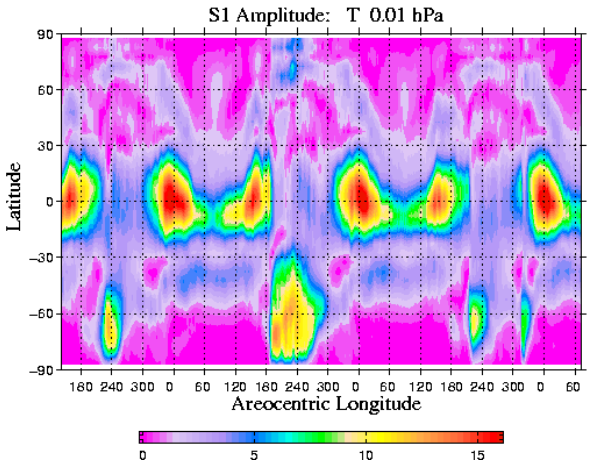

Figure 4. Seasonal variation of the migrating diurnal component of temperature (K) at 0.01 hPa. These results are derived from the TES Control simulation.

Diurnal tide: The seasonal variation of the amplitude of the migrating diurnal component of temperature is shown in Figure 4. There is a clear semiannual variation with prominent peaks in the equinoctial seasons. It has been noted [9,18] that the vertically propagating diurnal tide is ducted into the winter hemisphere and tend to dissipate at relatively low altitudes. This is particularly the case for stronger forcing (higher opacity). By contrast, the tropical tide propagates vertically to much greater heights in the equinoctial seasons. The migrating diurnal tide contributes to the zonal momentum balance of the tropical atmosphere, most notably at the equinoxes [19].

Near-Surface Winds: The diurnal variation of boundary layer winds has a large influence on Martian weather and tides likely figure prominently in control dust storm activity. The response is strongly influenced by atmospheric dust loading. In order to characterize the tide winds and the influence of topographic slope, we have used a least-squares technique to fit an ellipse to the hodograph describing the diurnal variation of U and V at each model gridpoint. Slope effects may be illustrated by determining the major and minor axes of the fitted ellipse and comparing the angle of the major axis with that of the local topographic slope. Scatter plots show that the lowest level winds have a very clear afternoon upslope character.

Figure 5 shows the seasonal variation of the zonally-averaged one kilometer altitude tide wind amplitude over the MGS mission. The figure shows the expected peaking of tide amplitude at subtropical latitudes. Of course, the spatial variability is more interesting. For example, Figure 6 shows the spatial distribution of tide wind amplitude at L_s = 221 in MY24.

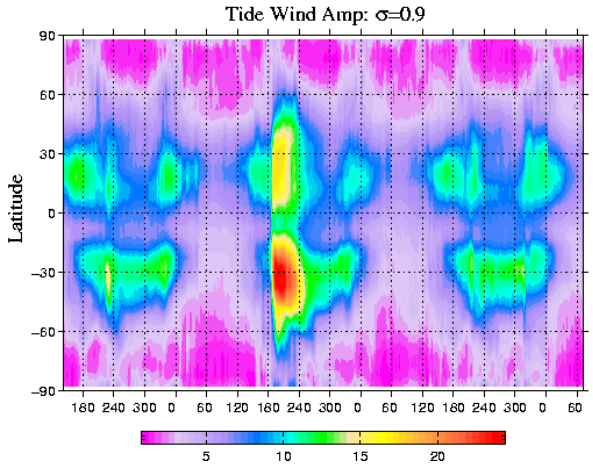

Figure 5. Seasonal variation of the tide wind amplitude at roughly 1 km above ground level. Units are ms^{-1}.

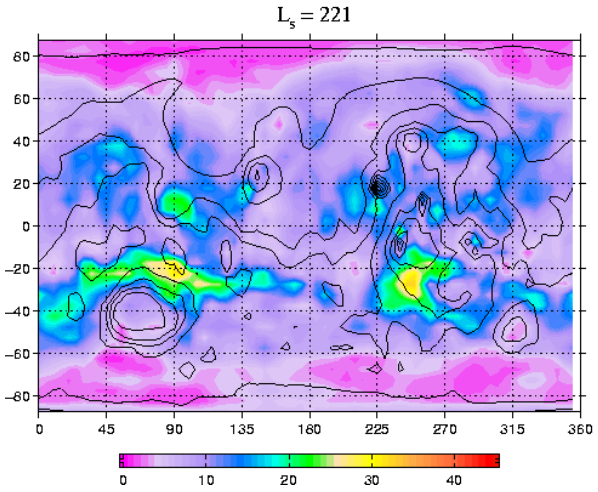

Figure 6. Spatial distribution of tide wind amplitude at one kilometer above ground.

Conclusions and Future work: We have found that the Kelvin wave component of diurnal surface pressure variability responds to zonal modulation in the thermal forcing associated with dust activity or water ice clouds. This has motivated the continuing investigate of the potential role of radiatively active water ice clouds in modifying the forcing of the diurnal Kelvin wave. Seasonal variations in dust activity are expected to have a significant influence on density structure at aerobraking altitudes. There are large changes in the tide winds in response to dust storm activity and topograply has a major influence on near-surface wind variability.

References:

[1] Banfield, D. et al. (2003) *Icarus*, 161, 319-345.
[2] Montabone, L. et al. (2005) *Adv. Space Res.*, *36*, 2146-2155.
[3] Montabone, L. et al. (2006) *Icarus*, *185*, 113-132.
[4] Lewis, S.R. et al. (2007) *Icarus*, *192*, 327-347.
[5] Montabone, L. et al. (2008) Abstract in this issue.
[6] Smith, M.D. (2004) *Icarus*, *167*(1), 148-165.
[7] Zurek, R.W. and C.B. Leovy (1981), *Science*, *213*, 437-439.
[8] Lewis., S.R., and P.R. Barker (2005) *Adv. Space Res.*, 36, 2162-2168.
[9] Wilson, R.J. and K.P. Hamilton (1996) *J. Atmos. Sci.*, ***53***, 1290-1326.
[10] Wilson, R.J. et al. (2008) *Geophys. Res. Lett.*, *35*, L07202, doi:10.1029/GL032405 [15] Wilson, R.J. (2000) *Geophys. Res. Lett.*, *27*, 3889-3892.
[11] Hinson, D. and R.J. Wilson (2004) *JGR*, *109*, E10002, doi:10.1029/JE002129.
[12] Wilson, R.J. et al. (2007) *Geophys. Res. Lett.*, *34*, L02710, doi:10.1029/2006GL027976.]
[13] Bridger, A.F.C., and J.R. Murphy (1998) *J. Geophys. Res.*, *103*, 8587-8601.
[14] Hinson, D. (2007), 7th international Mars meeting, Pasadena, CA.
[15] Wilson, R.J. (2002) *Geophys. Res. Lett.*, *29*, 10.1029/2001GL013975.
[16] Withers, P. et al. (2003) *Icarus*, *164*, 14-32.
[17] Angelats i Coll., M. et al. (2004) *JGR*, *109*, E01011, doi:10.1029/2003JE002163.
[19] Lewis, S.R. and P.L. Read (2003), *JGR*, 108, 10.1029/2002JE001933.
[18]Takahashi, Y.O. et al. (2006) *JGR* 111, E01003.